

Atomistic simulation of flow-induced crystallization at constant temperature

C. BAIG^{1(a)} and B. J. EDWARDS^{2(b)}

¹ *Department of Chemical Engineering, University of Patras & FORTH-ICE/HT - Patras, GR 26504, Greece, EU*

² *Department of Chemical and Biomolecular Engineering, University of Tennessee - Knoxville, TN 37996, USA*

received 13 October 2009; accepted in final form 25 January 2010

published online 23 February 2010

PACS 61.20.Ja – Computer simulation of liquid structure

PACS 36.20.Ey – Conformation (statistics and dynamics)

PACS 61.20.Gy – Theory and models of liquid structure

Abstract – Semi-crystalline fibers, such as nylon, orlon, and spectra, play a crucial role in modern society in applications including clothing, medical devices, and aerospace technology. These applications rely on the enhanced properties that are generated in these fibers through the orientation and deformation of the constituent molecules of a molten liquid undergoing flow prior to crystallization; however, the atomistic mechanisms of flow-induced crystallization are not understood, and macroscopic theories that have been developed in the past to describe this behavior are semi-empirical. We present here the results of the first successful simulation of flow-induced crystallization at constant temperature using a nonequilibrium Monte Carlo algorithm for a short-chain polyethylene liquid. A phase transition between the liquid and crystalline phases was observed at a critical flow rate in elongational flow. The simulation results quantitatively matched experimental X-ray diffraction data of the crystalline phase. Examination of the configurational temperature generated under flow confirmed for the first time the hypothesis that flow-induced stresses within the liquid effectively raised the crystallization temperature of the liquid.

Copyright © EPLA, 2010

Interest in semi-crystalline fibrous materials exploded after the discovery of nylon in 1935. Many novel crystalline fibers have since been produced and marketed under such household trade names as orlon, rayon, spectra, etc. Typical applications of these materials include clothing, fabrics, textiles, surgical instruments, military equipment, optical components, sensing devices, and many others; these materials are thus crucial to a vast number of consumer products and niche-market applications.

A chief property of semi-crystalline fibers is their mechanical toughness: the fibers are typically ten times stronger than steel on an equivalent-weight basis. This property is strongly dependent on the degree of orientation of the chain-like macromolecules within the fibers. Despite these materials representing a multi-billion dollar per year industry, very little is still known theoretically about the fundamental physics regarding orientation and subsequent crystallization of the chain molecules from the liquid state. This lack of knowledge is a significant barrier to the development of novel applications of these

materials because the morphology of the crystallized fibers under flow can be substantially different than that which is obtained under a quiescent temperature quench, and is highly dependent on the flow type and strength [1–5]. Thus the application of flow can be used as an effective means of tailoring the crystalline structure to specific applications if a sound theoretical background is available to guide intelligent design.

The primary method of obtaining the requisite degree of orientation in crystallized fibers is to stretch out and orient the constituent chain molecules prior to crystallization using an applied flow field, such as in an industrial-scale fiber-spinning operation, from either a polymer melt or solution. Much work has been directed over the past 50 years to understand this process, and several excellent reviews exist [1–3]. During the 1960s, the first direct rudimentary observations of flow-induced crystallization began to appear. The next decade of the 1970s brought greater sophistication to the experimental endeavors, with birefringence and dichroism playing a key role in determining the crystallization morphology and kinetics under flow. Recent advances in experimental methodology [6–9] have allowed investigation of the structural changes occurring

^(a)E-mail: cbaig@iceht.forth.gr

^(b)E-mail: bje@utk.edu

in polymeric systems during flow at various spatial and temporal scales.

The 1980s brought the first empirical macroscopic theories for flow-induced crystallization. Specifically, Rangel-Nafaile *et al.* [1] introduced a model based on the famous Flory-Huggins theory of mixtures that incorporated an additional phenomenological term that was proportional to the stress that developed within the flowing liquid. In this way, these authors were able to provide an empirical quantification of a hypothesis that the configurational changes introduced by the flowing stresses were effectively raising the melting temperature of the material under investigation by up to 28°C; this value was commensurate with some experimental observations [1,5].

In the 1990s, effort was devoted to further the development of macroscopic theories [10–12], but the models were still mostly empirical in nature, and achieved no quantitative agreement with experimental data. The 2000s produced the first statistical theories of flow-induced crystallization, but these microscopic models produced only a qualitative understanding of the phenomenon of flow-induced crystallization [13,14]. To date, no existing model has been able to confirm or deny the hypothesis that stresses generated under flow raise the melting point of a material by orienting and deforming the constituent macromolecules at constant temperature, and no explicit atomistic simulations based on first-principles, rather than a theoretical model, of flow-induced crystallization have been reported.

Atomistic simulation is an important tool for the study of crystallization kinetics and nucleation [15–18]. In particular, Rutledge and co-workers [15,16] carried out pioneering molecular dynamics (MD) studies on the crystallization process by applying an arbitrary large stress in one preferred direction to polyethylene liquids under both isothermal and nonisothermal conditions. They noted the important role of molecular mobility and local segmental rearrangement on the development of the crystalline phase. Although the previous work [15–18] has provided valuable fundamental information on the kinetics of nucleation and morphological developments at atomistic length scales, the physically artificial process of applying a one-dimensional stress, instead of a nonequilibrium flow process, makes their results are not directly applicable to flow-induced crystallization at constant temperature.

A nonequilibrium MD study of the *n*-alkane C₂₀H₄₂ was recently performed [19] which demonstrated that the local intramolecular structure of the liquid under a very strong steady planar elongational flow was quantitatively similar to that of the real crystal, obtained via X-ray diffraction, at short length scales; however, any sign of global long-range order existing in the real crystal was not detected, and all order disappeared quickly after cessation of flow. It is possible that the development of long-range order was retarded by the planar nature of the applied flow field,

which is of extension in the flow direction, compression in the perpendicular direction, and neutral in the third direction; *i.e.*, the neutral direction allows a significant degree of freedom with respect to molecular packing which is subject to intense thermal fluctuations. It is also possible that thermostat artifacts in the MD simulations at high strain rates played a role in the absence of the development of long-range crystalline order.

The two issues mentioned above can be overcome by performing nonequilibrium Monte Carlo (MC) simulations of a chain liquid under uniaxial flow. The uniaxial flow field has a higher degree of orienting power due to the fact that equal compression occurs in both perpendiculars to the extension direction, instead of just one as in planar elongational flow. Unfortunately, bulk uniaxial flow cannot be simulated at present using MD because of the absence of the requisite periodic boundary conditions. Also, no thermostat artifacts will disturb the system in an MC simulation.

The MC algorithm adopted in this work is a thermodynamically well-founded nonequilibrium Monte Carlo methodology [20] that has proven to be capable of generating realistic steady-state structures of flowing polymeric systems at various length scales [21,22]. The key to the nonequilibrium MC method is to determine proper structural variables that are able to represent effectively the deformed nonequilibrium states of system [20–22]. For the C₇₈H₁₅₈ linear polyethylene liquid with a small polydispersity index (≈ 1.083) examined in this work, with atomistic interactions defined by the potential (SKS) model of Siepmann *et al.* [23], an appropriate structural variable is the second-rank conformation tensor $\tilde{\mathbf{c}} = 3\langle \mathbf{R}\mathbf{R} \rangle / \langle R^2 \rangle_{\text{eq}}$. Here \mathbf{R} denotes the chain end-to-end vector and the angular brackets denote ensemble averages. With this method, it was possible to impose a strong, steady-state uniaxial elongational flow to the liquid system through the conjugate thermodynamic field variable $\boldsymbol{\alpha}$ (of second-rank) with respect to $\tilde{\mathbf{c}}$; *i.e.*, $\alpha_{yy} = \alpha_{zz} = -\frac{1}{2}\alpha_{xx}$, with all the off-diagonal components being zero [23]. A broad range of α_{xx} [0.0,1.0] (see ref. [24] for the applicable range of Weissenberg number, Wi) was applied to each system at a fixed density of $\rho = 0.7638 \text{ g/cm}^3$. Four different temperatures (300, 350, 400, and 450 K) were studied. Long MC cycles with highly efficient moves and a large system size were used in the simulations to attain good statistics, to avoid any system-size effects, and to ensure the full attainment of steady states. The melt system was prepared with 160 linear C₇₈H₁₅₈ molecules in a rectangular box (enlarged in the stretching (x) direction) with the dimensions ($x \times y \times z$ in units of Angstroms) of $130.5 \times 54 \times 54 \text{ \AA}^3$. This box dimension was chosen to be large enough to avoid any undesirable system-size effects (especially under strong flow fields), based on the fully stretched chain length (*i.e.*, with the equilibrium C-C bond length (1.54 Å) and C-C-C bending angle (114°) in the all *trans*-conformation). The maximum length of the

end-to-end vector $|\mathbf{R}|_{\max} = 99.4 \text{ \AA}$, and the mean chain end-to-end distance at equilibrium $\langle R^2 \rangle_{\text{eq}}^{1/2} = 39.3 \pm 0.5 \text{ \AA}$ for the $\text{C}_{78}\text{H}_{158}$ melt at $T = 450 \text{ K}$ and $\rho = 0.7638 \text{ g/cm}^3$. Hence, the x dimension of the simulation box was at least 30% larger than the $|\mathbf{R}|_{\max}$ value, and similarly for the y and z dimensions based on the value of $\langle R^2 \rangle_{\text{eq}}^{1/2}$. A well-equilibrated initial configuration was prepared for each simulation.

The effects of flow on the liquid conformation were analyzed in terms of the structure factor $S(k)$, which was obtained via Fourier transformation of the pair correlation function $g(r)$ (fig. 1). At equilibrium (*i.e.*, $\alpha_{xx} = 0$), all temperatures displayed a similar isotropic, amorphous structure over the whole range of k (inset, fig. 1(a)), displaying a relatively weak temperature dependence on both the average intramolecular configuration (reflected in high k -regimes, *i.e.*, $k > 6 \text{ \AA}^{-1}$) and the intermolecular ordering (reflected in low k -regimes, *i.e.*, $k < 6 \text{ \AA}^{-1}$) of the liquid. Also included in the inset is the structure factor as determined via X-ray measurements for liquid n -eicosane, $\text{C}_{20}\text{H}_{42}$ at 315 K [25] (represented by the circles). In spite of the difference in size between the simulated liquid and the real one (*i.e.*, 78 carbon atoms as opposed to 20), the agreement between the two sets of data is excellent, thus providing a degree of confidence in the accuracy of the SKS potential model that was used in the simulations.

In sharp contrast, highly anisotropic structures were observed in nonequilibrium systems under strong flow fields (main graph, fig. 1(a)). At the two highest temperatures, 400 and 450 K, the chain molecules have become highly extended and anisotropic, which is evident from the shift in peaks at high k values from the equilibrium structure represented in the inset. However, at low values of k , no long-range crystalline order was evident, indicating that although the molecules were dramatically oriented and elongated under flow, no true flow-induced crystallization was occurring. Indeed, after cessation of flow, the molecules at these two higher temperatures returned to their quiescent isotropic structures, as displayed in fig. 2 (this behavior was also observed by Ionescu *et al.* [19]), where a relaxation simulation was performed for each system by turning off the applied field after the systems reached the steady states at $\alpha_{xx} = 1.0$ in order to examine the nature of the flow-induced crystalline created in the systems at $T = 350$ and 300 K , compared to the simply oriented melts at $T = 450$ and 400 K . The results are shown in terms of the mean-square chain end-to-end distance (normalized by its equilibrium value) (fig. 2). Clearly, the oriented melt phases in the systems at $T = 450$ and 400 K disappear quickly after removing the field. In contrast, the crystalline phase in the systems at $T = 350$ and 300 K appeared to continue its state in a stable manner. This result directly illustrates the intrinsic difference between the two phases.

At $T = 350$ and 300 K , distinct Bragg peaks became evident at small values of k ($< 1.5 \text{ \AA}^{-1}$) representing a long-range order, typical of a real crystal (fig. 1(a)). After

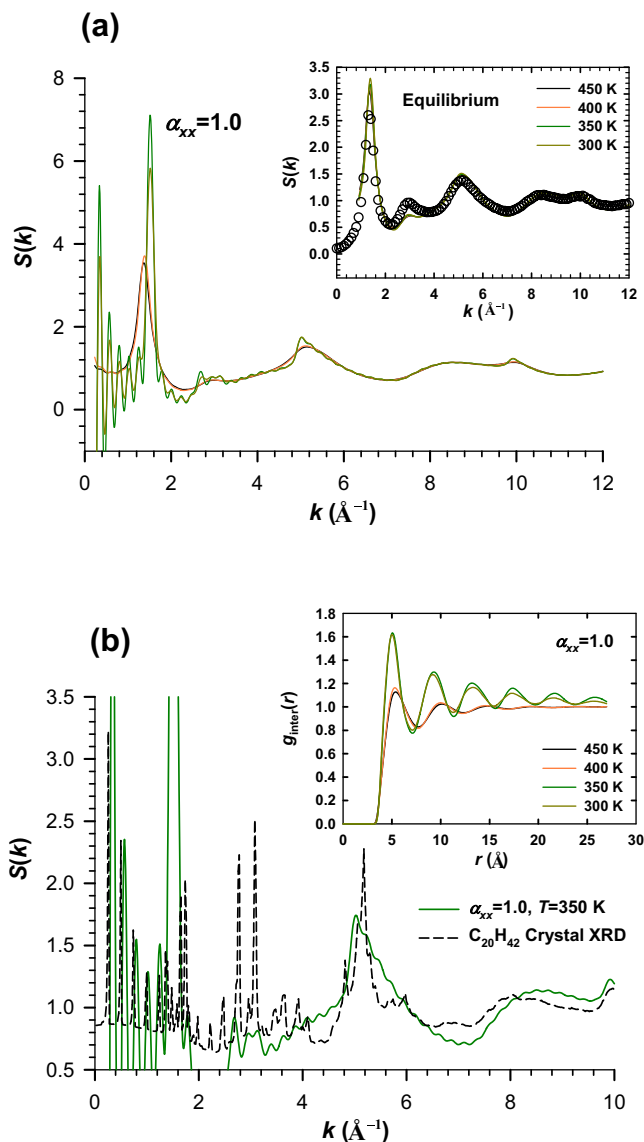


Fig. 1: (Color online) Structure factors of the equilibrium and the elongated melts. The bin sizes of the wavenumber k used in the calculations was 0.01 \AA^{-1} . (a) Comparison between the liquid structures at different temperatures at equilibrium ($\alpha_{xx} = 0$) (inset) and under uniaxial flow ($\alpha_{xx} = 1.0$) (main graph). Circles within the inset represent X-ray data of liquid n -eicosane at 315 K. (b) Comparison between the flow-induced crystalline structure created in the system at $T = 350 \text{ K}$ and the X-ray diffraction data of the crystal n -eicosane. The inset shows the intermolecular part of $g(r)$ for each temperature at $\alpha_{xx} = 1.0$.

cessation of flow, these structures remained for a long time, rather than quickly decaying back to the equilibrium structure of the quiescent melts (fig. 2). Additional features supportive of the flow-induced crystalline phase were the shift of the main peak at $k \approx 1.38 \text{ \AA}^{-1}$ occurring in equilibrium liquids to larger $k \approx 1.52 \text{ \AA}^{-1}$ (indicating a closer lateral packing between neighboring chains) and the broken symmetry of the peak at $k \approx 5 \text{ \AA}^{-1}$.

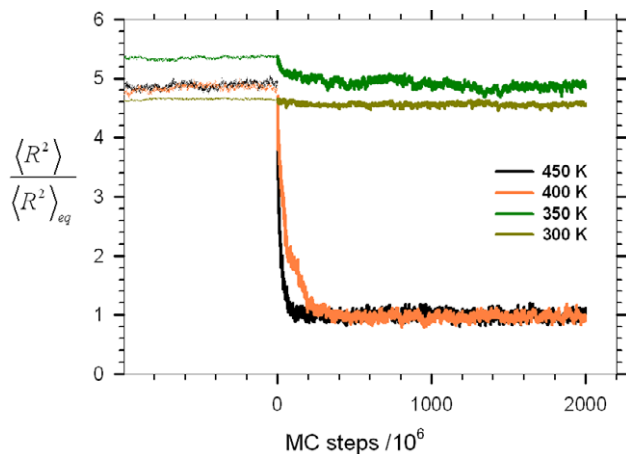


Fig. 2: (Color online) Relaxation behaviors (depicted by the thick solid lines that begin at the MC step equal to zero) of system in terms of the mean-square chain end-to-end distance $\langle R^2 \rangle$ after turning off the flow field. Each system was subjected to the flow field of $\alpha_{xx} = 1.0$ and fully attained the steady state (depicted by the thin dotted lines) before removing the field (*i.e.*, $\alpha_{xx} = 0$). The $\langle R^2 \rangle_{eq}$ were found to be equal to $1547 \pm 20 \text{ \AA}^2$ for $T = 450 \text{ K}$, $1679 \pm 23 \text{ \AA}^2$ for $T = 400 \text{ K}$, $1793 \pm 22 \text{ \AA}^2$ for $T = 350 \text{ K}$, and $2087 \pm 30 \text{ \AA}^2$ for $T = 300 \text{ K}$.

Further quantitative examination of the flow-induced crystalline (FIC) structure can be made using fig. 1(b), where the simulated structure is compared directly with the experimental X-ray data for the *n*-eicosane crystal, indexed as triclinic, from ref. [19]. There is a remarkable quantitative match of the Bragg peaks below $k = 1.4 \text{ \AA}^{-1}$, confirming the existence of regular intermolecular crystal planes in the FIC phase, as well as above 6 \AA^{-1} , indicating intramolecular configurations very close to those in the actual crystal. In the intermediate range, $2 < k < 6 \text{ \AA}^{-1}$, the three distinct crystalline Bragg peaks at 2.7 , 3.1 , and 5.2 \AA^{-1} , are much less pronounced in the simulation data, indicating that the FIC phase has a slightly different morphology than the quiescently crystallized sample, which is consistent with experiment [1–5]. The essential order of the real crystal is thus preserved in the simulated FIC phase, with respect to the intramolecular configurations and lateral intermolecular chain packing, but the smeared-out Bragg peaks in the simulation data indicate that the packing in the longitudinal direction is not as dramatic as in the true crystal.

More evidence of a FIC phase in the simulation data is provided by examining the intermolecular contribution to $g(r)$ (inset, fig. 1(b)). Here, a distinct, long-range periodic order at the lower two temperatures is evident out to the maximum distance that could be analyzed given the dimensions of the simulation cell. A general rule of thumb in amorphous polymers is that significant crystalline structure has developed when a periodic structure exists out to roughly $25\text{--}30 \text{ \AA}$. Note that at the higher two temperatures, the periodicity has decayed by 15 \AA , indicating the lack of long-range order.

In 1974, de Gennes [26] introduced the concept of the “coil-stretch transition” in molecular configurations; *i.e.*, a sharp or discontinuous increase in the molecular extension occurring under the application of an external field. Figure 3(a) presents simulation data at the four temperatures of the mean fractional chain extension *vs.* flow strength. At the higher two temperatures, the extension shows a sharp but continuous increase at intermediate values of α_{xx} , indicating a smooth transition from the coiled to the stretched configuration. However, at 350 and 300 K, abrupt and seemingly discontinuous transitions were observed at critical values of flow strength corresponding to 0.3 and 0.2, respectively. After the critical value has been obtained, further increase in flow strength has little effect on the average chain extension, which is very close to the maximum attainable value of unity.

The abrupt transition is further reflected in the enthalpy change with flow strength presented in fig. 3(b). At the lower two temperatures, there is again a discontinuous change in the enthalpy of the FIC phase relative to the equilibrium state, and the ultimate values of ΔH are much greater than in the liquid state, where the enhanced orientation leads to relatively minor changes in this quantity. As an interesting point, note that the value of ΔH at $\alpha_{xx} = 1$ (225 J/g) is remarkably close to the experimental heat of fusion (276 J/g) of a polyethylene crystal [27], further indicating a FIC phase has been achieved. We further report that the sudden transition in ΔH has also been observed in the Helmholtz free energy change ΔA (obtained by thermodynamic integration with respect to α , starting from the equilibrium melt (*i.e.*, $\alpha = \mathbf{0}$); refer to eq. (17) in ref. [22]) at the lower temperatures (300 and 350 K), whereas at the higher-temperature liquids (400 and 450 K) it increases continuously with the flow strength; in addition, ΔA is found to be much smaller at the lower temperatures than the higher temperatures, indicating that the FIC phase created under strong flow fields is a quite stable thermodynamic state compared to the equilibrium melt.

During the previous decade, Rugh [28] discovered that temperature could be calculated from the atomistic configuration only, not just with respect to the atomistic kinetic energy; this quantity was thus called the “configurational temperature,” T_{conf} . Although strictly valid only under equilibrium conditions, this idea can be extended to flowing systems by invoking the assumption of a local or quasi-thermodynamic equilibrium, which is standard protocol in the theory of nonequilibrium thermodynamics [29]. Using T_{conf} , structural changes of the system in response to external flow fields can be related to the theoretical temperature that the molecules effectively experience with regard to chain configurations and ordering, even though the actual temperature of the simulation has not changed. The plots of T_{conf} *vs.* $\text{tr}(\hat{c})$ for the four temperatures are presented in fig. 4, where a monotonic decrease of T_{conf} is evident in each case. This indicates that the molecules are extending, orienting, and packing into structures that they would be assuming at lower actual

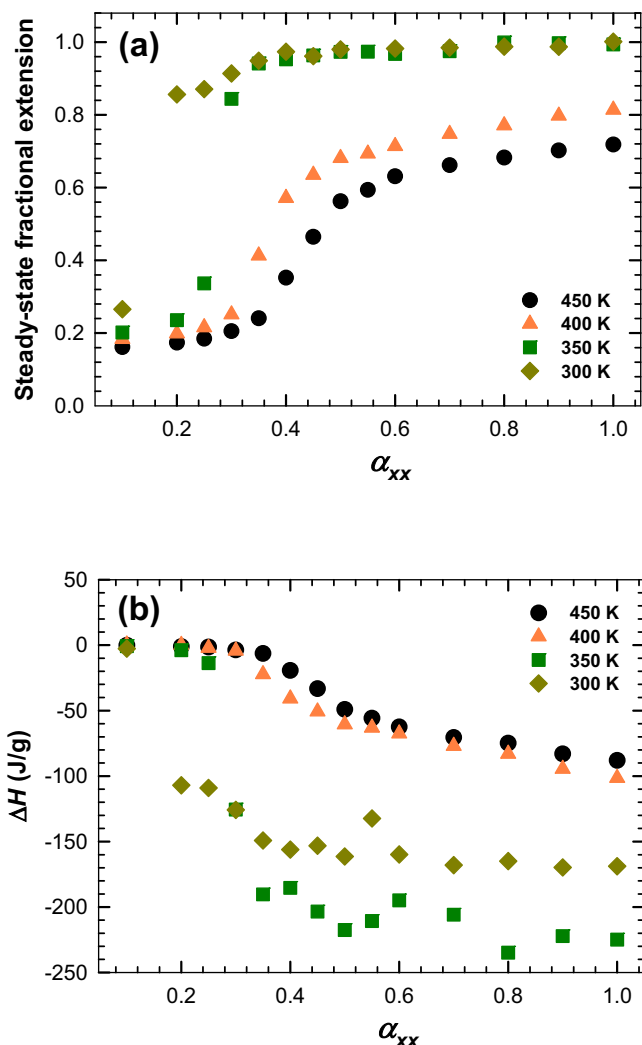


Fig. 3: (Color online) (a) Average fractional polymer extension as a function of the field strength for each temperature. The fraction was calculated as the ratio of average chain extension relative to the maximum extension ($|\mathbf{R}|_{\max} = 99.4 \text{ \AA}$) of a linear $C_{78}H_{158}$ molecule in the full *trans*-conformation with the equilibrium C-C bond length (1.54 \AA) and C-C-C bending angle (114°). (b) Enthalpy change $\Delta H (= H_{\text{noneq}} - H_{\text{eq}})$ between equilibrium and nonequilibrium states with respect to flow strength. The standard errors are commensurate with the size of the symbols.

temperatures. Indeed, at 350 and 300 K, the decrease is very dramatic, and discontinuous at the critical values of Wi , providing a further indication of flow-induced crystallization. This observation is consistent with the hypothesis that the stresses applied under flow effectively raise the crystallization temperature of the liquid state [1]. The experimentally reported $15\text{--}20^\circ\text{C}$ increase of T_m for a polyethylene crystal [6] compares well with the simulated value of $\sim 13^\circ\text{C}$ decrease of T_{conf} at $T = 350 \text{ K}$.

In summary, atomistic simulations of a flow-induced crystalline phase from an isotropic liquid by application of a uniaxial elongational flow field have been performed using nonequilibrium Monte Carlo methodology. The FIC

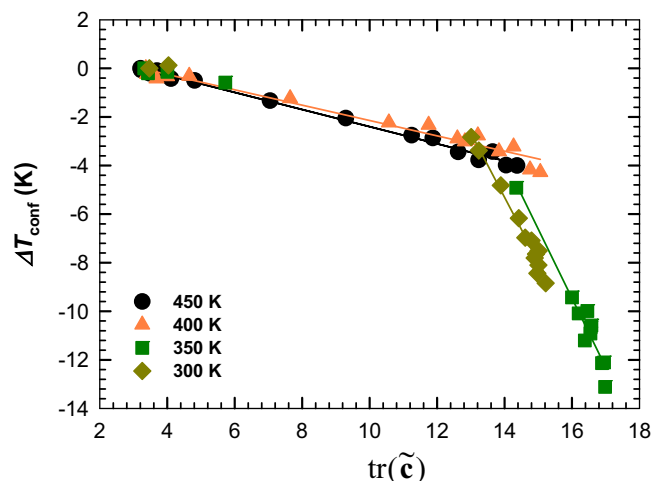


Fig. 4: (Color online) The configurational temperature change $\Delta T_{\text{conf}} (= T_{\text{conf,noneq}} - T_{\text{conf,eq}})$ vs. $\text{tr}(\tilde{\mathbf{c}})$. The solid lines represent the linear fit of the data for each set-point temperature. Fitting to $\Delta T_{\text{conf}}/T_{\text{eq}} = E \text{tr}(\tilde{\mathbf{c}})$, E was found to be $(-7.8 \pm 0.2) \times 10^{-4}$ for $T = 450 \text{ K}$ and $(-7.9 \pm 0.4) \times 10^{-4}$ for $T = 400 \text{ K}$ for the melt phase, and $(-8.1 \pm 0.6) \times 10^{-3}$ for $T = 350 \text{ K}$ and $(-8.8 \pm 0.4) \times 10^{-3}$ for $T = 300 \text{ K}$ for the crystalline phase; therefore, within statistical uncertainties, a common slope was found for each phase.

structure was found to have a global long-range order, as observed in real crystals. The sharp Bragg peaks at small k values and the long-range local density correlation in the FIC phase clearly demonstrated the primary characteristics of real crystallites. Furthermore, the simulations confirmed the long-standing hypothesis that flow-induced stresses within the liquid effectively raised the crystallization temperature of the liquid (the melting point elevation under flow). The conformation tensor based on the chain end-to-end vector is shown to be well qualified as a proper thermodynamic state variable for representing the overall structure of short-chain liquids in nonequilibrium states. (Analogously, in the nonequilibrium MC method developed by Rutledge and co-workers, the orientation distribution functions at different length-scales have been employed as a state variable [30].) For long-chain entangled polymeric systems, more detailed physical measures (*e.g.*, local conformation tensor based on each entanglement strand or the Doi-Edwards orientational distribution function) can also be considered as the nonequilibrium state variables; efforts are currently in progress in this direction. At the same time, it is necessary to consider carefully in the data analysis the approximations involved in each coarse-grained mapping MC procedure simulating the flow field; *e.g.*, effective length-scales, lack of dynamics, and the empirical (or model-dependent) relation between the thermodynamic variables and the flow field.

This work was supported by the National Science Foundation under Grant No. CBET-0742679.

REFERENCES

- [1] RANGEL-NAFAILE C., METZNER A. B. and WISSBRUN K. F., *Macromolecules*, **17** (1984) 1187.
- [2] KELLER A. and MACHIN M. J., *J. Macromol. Sci., Part B: Phys.*, **1** (1967) 41.
- [3] MCHUGH A. J. and FORREST E. H., *J. Macromol. Sci., Part B: Phys.*, **11** (1975) 219.
- [4] MACKLEY M. R. and KELLER A., *Polymer*, **14** (1973) 16.
- [5] SIEGLAFF C. L. and O'LEARY K. J., *Trans. Soc. Rheol.*, **14** (1970) 49.
- [6] SOMANI R. H., YANG L., ZHU L. and HSIAO B. S., *Polymer*, **46** (2005) 8587.
- [7] MCHUGH A. J., GUY R. K. and TREE D. A., *Colloid Polym. Sci.*, **271** (1993) 629.
- [8] RIETVELD J. and MCHUGH A. J., *J. Polym. Sci. Part B: Polym. Phys.*, **23** (1985) 2339.
- [9] KIMATA S. *et al.*, *Science*, **316** (2007) 1014.
- [10] BUSHMAN A. C. and MCHUGH A. J., *J. Polym. Sci. Part B: Polym. Phys.*, **34** (1996) 2393.
- [11] DOUFAS A. K., DAIRENIEH I. S. and MCHUGH A. J., *J. Rheol.*, **43** (1999) 85.
- [12] ZUIDEMA H., PETERS G. W. M. and MEIJER H. E. H., *Macromol. Theory Simul.*, **10** (2001) 447.
- [13] DOUFAS A. K., MCHUGH A. J. and MILLER C., *J. Non-Newtonian Fluid Mech.*, **92** (2000) 27.
- [14] MUKHERJEE J., WILSON S. and BERIS A. N., *J. Non-Newtonian Fluid Mech.*, **120** (2004) 225.
- [15] LAVINE M. S., WAHEED N. and RUTLEDGE G. C., *Polymer*, **44** (2003) 1771.
- [16] KO M. J., WAHEED N., LAVINE M. S. and RUTLEDGE G. C., *J. Chem. Phys.*, **121** (2004) 2823.
- [17] DUKOVSKI I. and MUTHUKUMAR M., *J. Chem. Phys.*, **118** (2003) 6648.
- [18] HU W., FRENKEL D. and MATHOT V. B. F., *Macromolecules*, **35** (2002) 7172.
- [19] IONESCU T. C., BAIG C., EDWARDS B. J., KEFFER D. J. and HABENSCHUSS A., *Phys. Rev. Lett.*, **96** (2006) 037802.
- [20] MAVRANTZAS V. G. and ÖTTINGER H. C., *Macromolecules*, **35** (2002) 960.
- [21] BAIG C. and MAVRANTZAS V. G., *Phys. Rev. Lett.*, **99** (2007) 257801.
- [22] BAIG C. and MAVRANTZAS V. G., *Phys. Rev. B*, **79** (2009) 144302.
- [23] SIEPMANN J. I., KARABONI S. and SMIT B., *Nature*, **365** (1993) 330.
- [24] The Weissenberg number (Wi) represents the ratio of elastic to kinematic forces within a flowing liquid. An empirical relation between α and Wi for the same chain liquid under shear flow was reported in ref. [22], based on the conformation tensor $\tilde{\mathbf{c}}$. Using a similar procedure and comparing for $\tilde{\mathbf{c}}$ with previous nonequilibrium MD data of $C_{78}H_{158}$ at the same T and ρ under planar elongational flow (BAIG C. *et al.*, *J. Chem. Phys.*, **124** (2006) 084902), this range of α_{xx} is approximately estimated to imply $0.1 \leq Wi \leq 200$.
- [25] HABENSCHUSS A. and NARTEN A. H., *J. Chem. Phys.*, **92** (1990) 5692.
- [26] DE GENNES P. G., *J. Chem. Phys.*, **60** (1974) 5030.
- [27] GAUR U. and WUNDERLICH B., *J. Phys. Chem. Ref. Data*, **10** (1981) 119.
- [28] RUGH H. H., *Phys. Rev. Lett.*, **78** (1997) 772.
- [29] BERIS A. N. and EDWARDS B. J., *Thermodynamics of Flowing Systems* (Oxford University Press, New York) 1994.
- [30] BERNARDIN F. E. and RUTLEDGE G. C., *Macromolecules*, **40** (2007) 4691.